

## Fluvial aggradation in Vedder River: Testing a one-dimensional sedimentation model

R. I. Ferguson

Department of Geography, Sheffield University, Sheffield, England, UK

M. Church and H. Weatherly<sup>1</sup>

Department of Geography, University of British Columbia, Vancouver, British Columbia, Canada

**Abstract.** Sediment routing models which simulate the coevolution of river long profile and bed grain size distributions have been used to investigate downstream fining above base level, channel response to rectification, and other disequilibrium situations at a variety of timescales. We extend one such model (SEDROUT [Hoey and Ferguson, 1994]) to deal with sand as well as gravel and test its ability to simulate aggradation and downstream fining in a well-documented Canadian river. Previous tests of this and similar models have been largely restricted to comparing observed and simulated gradients of downstream fining, but it is not obvious when to make the comparison in a time-dependent model with uncertain initial state and no equilibrium except in the very long term. We discuss and apply a more rigorous set of test criteria and address issues of defining initial conditions and time to test. The model's varying sensitivity to different boundary conditions and parameters indicates key data constraints on the testability and predictive accuracy of any such model. We also consider the adequacy of one-dimensional calculations in channels with variable width and present initial results of attempts to allow for this.

### 1. Introduction

Geomorphologists commonly assume that alluvial rivers are in a quasi-equilibrium state with morphology and slope adjusted so that the river has just the capacity to transport the load supplied from upstream. However, many channels are not in equilibrium. In particular, progressive aggradation is typical where rivers are approaching either their final base level (the sea or the junction with a much larger river) or some local base level. Local base levels occur at bedrock controls, where narrow valleys are partly blocked (e.g., by tributary fans, landslides, or moraines), where rivers emerge abruptly from mountains onto flatter terrain (e.g., grabens, glacial troughs, or coastal plains), and where rivers flow into natural or artificial lakes. Gravel or gravel/sand mixtures deposited by aggrading rivers are commonly sorted by size so that the deposit, hence the channel bed, fines downstream on the declining gradient. The development of downstream fining increases distal sediment flux because the threshold stress to mobilize the bed is reduced. This promotes progradation, with the deposit gradually extending downstream as well as building up in the proximal zone. Both the long profile of the channel and the downstream fining gradient evolve over time.

Numerical modeling is potentially a powerful way to investigate the time-dependent behavior of river channels. Models of the transport and deposition of different size fractions of bed material have been developed by several research groups

(e.g., MIDAS [van Niekerk *et al.*, 1992], SEDROUT [Hoey and Ferguson, 1994], and the model of Cui *et al.* [1996]). These are one-dimensional (1-D) models that use width-averaged representations of channel hydraulics, bedload transport, and aggradation or degradation in an iterative computational scheme. At each time step the bed elevation and grain-size distribution (GSD) are updated. Since the models track size fractions, the textural stratigraphy of the deposit is also estimated.

This paper applies SEDROUT to study the development of the long profile and sediment fining in Vedder River, southwestern British Columbia, Canada. There is little critical experience of transferring sediment routing models to different situations and scales, and the ability to test such models is often limited. SEDROUT was originally tested only on Allt Dubhaig, a small aggrading stream in Scotland, United Kingdom. For lack of firm knowledge of initial conditions, timescale, and therefore rate of development the test was mainly a visual comparison of observed and simulated amount of downstream fining, supported by evidence from field process measurements that the degree of size selectivity in the model was appropriate [Hoey and Ferguson, 1994]. Cui *et al.* [1996] also simulated the development of downstream fining during aggradation but were able to compare both pattern and rate by using results of a flume experiment with known initial conditions and simple steady boundary conditions. Talbot and Lapointe [2001] used SEDROUT to simulate the consequences of straightening a meandering reach and obtained encouraging results for both patterns and amounts of degradation and armoring over a known time interval. However, there has not yet (to our knowledge) been a thorough quantitative test of any model's ability to simulate both patterns and rates of aggradation and fining in a natural gravel bed river. The morphological, sediment, and process data available for Vedder River allow a test of

<sup>1</sup>Now at Kerr Wood Leidal Associates, North Vancouver, British Columbia, Canada.

SEDROUT in a river about 10 times wider than Allt Dubhaig, including comparison of process rates and thus the temporal accuracy of the model.

In this paper we make significant extensions to both the model itself and the procedures used to assess it. SEDROUT originally described the transport and deposition only of gravels, but is now extended to include the sand component of bedload. We also discuss how to compare a time-dependent model with present-day observations; study the dependence of model results on the specified initial conditions in an attempt to develop a general and unbiased model startup procedure; and investigate sensitivity to how the hydrological and sediment-supply forcing is specified. These matters have implications for the testability and predictive accuracy of all such models but have received scant attention in the literature.

## 2. SEDROUT Model

### 2.1. Overview

SEDROUT is one of several similar numerical models that simulate the coevolution of long profile and bed texture in an alluvial channel. Full details are given by *Hoey and Ferguson* [1994] and where necessary later in this paper, so only an overview is given here. Like MIDAS and the model of *Cui et al.* [1996] it was developed with long timescales in mind, to study the pattern of sedimentation and fining that develops over a large number of different-sized flood events rather than the short-term processes in a particular event. All three models treat flow properties and bedload transport on a width-averaged basis, solving the shallow-water equations for mean depth, water surface slope, and thus mean shear stress at a series of cross sections. The shear stress values are used to compute bedload transport capacity for each of many size fractions taking account of their current availability in the bed. Computed capacities are then compared with supply from upstream, bed elevation is updated using the overall sediment continuity equation, and bed grain-size distribution (GSD hereafter) is updated using a fractional continuity equation.

Where sediment routing models differ is in the choice of equations for flow resistance, fractional transport, and fractional continuity. The default choices in SEDROUT are a Keulegan-type logarithmic resistance law  $(1/f)^{0.5} = a \log(R/D_{84}) + b$  (where  $f$  is the Darcy-Weisbach friction factor and  $R$  is the hydraulic radius); *Parker's* [1990] gravel transport equations; and *Hoey and Ferguson's* [1994] generalization of *Parker and Sutherland's* [1991] fractional continuity equation. Each of these, and their equivalents in other models, involves one or more parameters. In any particular application of a model these parameters must be specified, together with initial and boundary conditions. The necessary initial conditions are the bed elevation and GSD at each cross section. The necessary boundary conditions are water discharge (possibly increasing downstream but usually assumed steady) and the sediment flux and GSD into the head of the channel and at any lateral inputs.

### 2.2. Fractional Transport

Bedload transport capacity is calculated in SEDROUT using the "ACRONYM" equations of *Parker* [1990], which were calibrated to measurements of gravel transport in Oak Creek, Oregon. *Parker's* equations predict the transport rate of each half-phi size fraction from its volumetric abundance in the bed surface layer and the applied shear stress. The quasi-threshold

"reference" stress for each fraction increases slightly with diameter via a hiding function, so transport is slightly size-selective.

Although Oak Creek contains sand, *Parker's* analysis was restricted to gravel, and *Cui et al.* [1996] accordingly excluded sand from their model. The presence of sand is an emerging issue in the behavior of gravel bed rivers [e.g., *Wilcock*, 1998], and for the present study we extended SEDROUT to include sand fractions down to a supposed suspension threshold of 0.25 mm. Extending *Parker's* equations to sand fractions requires three assumptions: (1) the form of the relationship between fractional transport rate and relative shear stress is the same for sand sizes as for gravel, (2) the hiding function fitted to Oak Creek gravel data extends to more poorly sorted gravel-sand beds, and (3) the "straining function" *Parker* introduced to correct for the changing surface/subsurface difference in GSD at higher stresses works adequately for a more poorly sorted bed.

The flume results of *Kuhnle* [1993] and *Wilcock* [1993] cast doubt on the adequacy of a single hiding function for strongly bimodal gravel/sand beds, but field and flume results for gravel beds with minor sand tails suggest that a single transport curve and hiding function can be used [*Ashworth and Ferguson*, 1989; *Wilcock*, 1992; *Wathen et al.*, 1995]. The bed of the unchanneled part of Vedder River contains no more than 30% sand even in subsurface samples, and relatively little on the surface, so we considered the retention of *Parker's* [1990] equations to be justifiable. But the third assumption is more problematic. ACRONYM uses a three-part relation between dimensionless transport rate and the shear stress ratio  $\varphi = \tau^*/\tau_r^*$ , based on the equations of *Parker et al.* [1982], who used the subsurface GSD. The transport rate is then multiplied by a straining factor  $\omega$  which allows for the anticipated change in surface GSD with changing stress: less coarse and less well sorted at higher stress [*Parker*, 1990, p. 425]. Sorting for this purpose is quantified using the psi ( $\psi$ ) standard deviation  $\sigma$ , where  $\psi = \log_2(D/\text{mm})$ . Lookup tables in ACRONYM embody the  $\sigma$ - $\varphi$  and  $\omega$ - $\varphi$  curves found for Oak Creek. The straining function is an attempt to generalize them to other channels with surface GSDs which are more or less well sorted than Oak Creek. It is assumed that uniform sediment requires no straining since its GSD cannot alter with stage, thus  $\omega \rightarrow 1$  as  $\sigma \rightarrow 0$ . *Parker* [1990] adopted the simplest possible function which satisfies Oak Creek and the uniform case: the linear relationship  $\omega = 1 + (\omega_o - 1)(\sigma/\sigma_o)$ , where the  $o$  subscript denotes a value from the Oak Creek curves and unsubscripted variables are for the new situation. When this straining function is used in SEDROUT for gravel-sand beds, which almost invariably are poorly sorted with  $\sigma > 2$  or even  $>3$ , anomalies arise which can lead to stalling of a simulation. In the case of the mean bed diameter, the curve of transport rate against stress develops an inflexion at  $\sigma > 1.6$  and a downturn at  $\sigma > 2.1$ , with zero transport at high stress when  $\sigma > 2.6$ . In an attempt to overcome this problem we tested a modified straining function added to SEDROUT by T. Hoey (personal communication, 1997):  $\omega = 1 + (\omega_o - 1)\sigma^{0.3}/\sigma_o$ . The reduced dependence on  $\sigma$  gives more stable results for poorly sorted beds, with a transport curve close to that for Oak Creek. An alternative, more general, formulation is  $\omega = 1 + (\omega_o - 1)(\sigma/\sigma_o)^c$  where  $c$  lies between 0 (no straining) and 1 (*Parker* straining);  $c$  has to be  $<0.4$  for reasonable behavior in poorly sorted beds.

The other parameters in ACRONYM were left at their default values in runs reported here. Increasing the reference

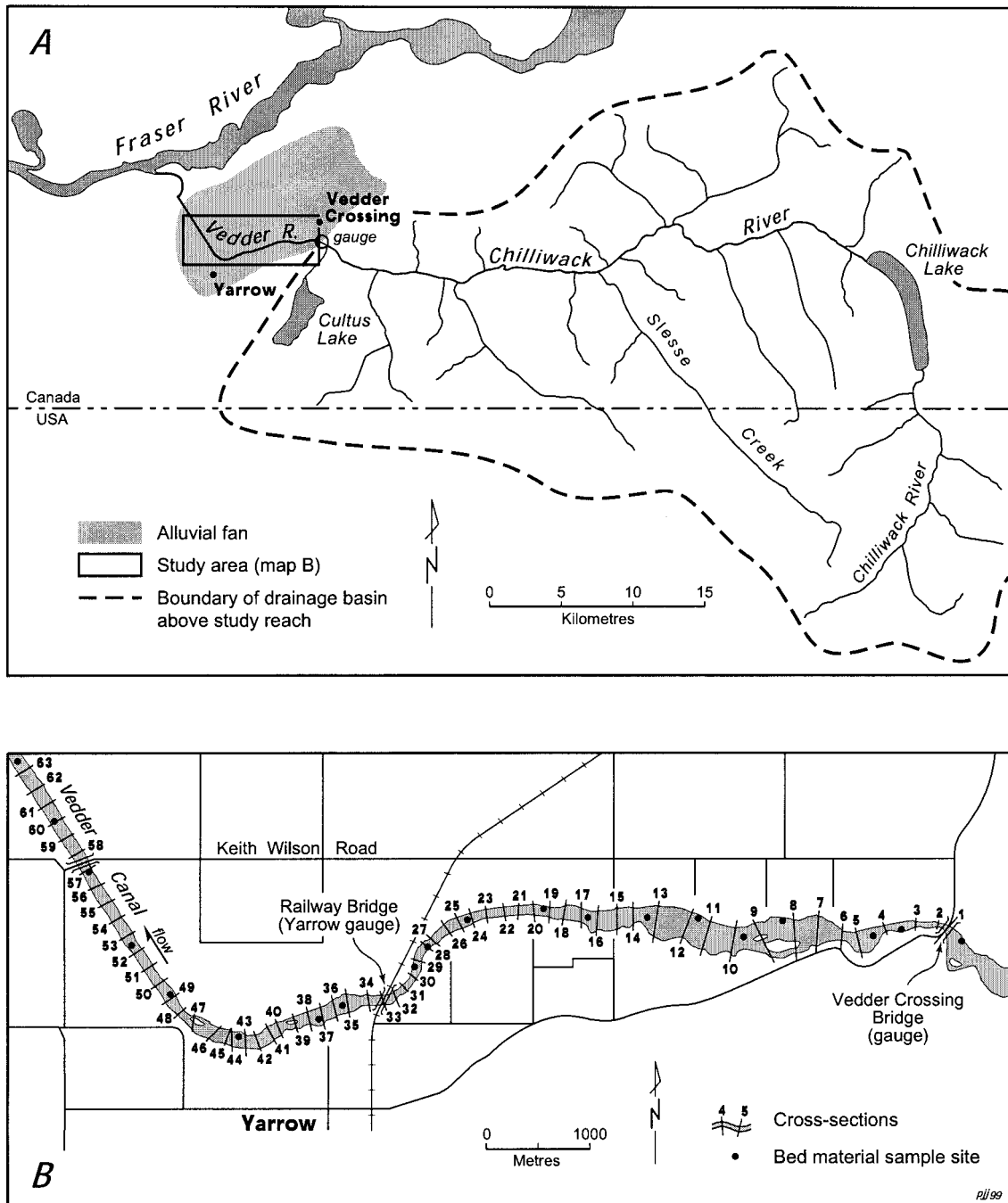


**Figure 1.** Chilliwack valley and the Vedder River study reach. Locations of model cross sections, bed material samples, and the Vedder Crossing gauge are shown. The numbering of cross sections 1–49 is reversed from that of *Martin and Church* [1995] (which corresponded with the original survey) because of enumeration conventions in the SEDROUT program.

Shields stress for bed  $D_{50}$  has the same effect as reducing the discharge. Altering the default value of 0.095 for the hiding factor affects the strength of downstream fining (weaker the closer to the equal-mobility value of 0). Sensitivity analysis confirmed the finding of *Hoey and Ferguson* [1997] that, within the plausible range of values (say 0.2 to 0.05), the effect is not great. Nevertheless, subtle adjustment of this parameter in combination with the treatment of GSD can influence the pattern of downstream fining.

### 3. Field Site and Data

Vedder River is a distal reach of Chilliwack River (Figure 1), draining 1230 km<sup>2</sup> of the Cascade Mountains approximately 160 km east of Vancouver. The river emerges at Vedder Crossing from a mountain valley onto an aggrading alluvial fan, where it is referred to as Vedder River. After a further 8 km, the river has been channelized and is referred to locally as Vedder Canal. Gravel delivered by Chilliwack River is depos-

ited on the alluvial fan in the Vedder River reach, with pebble gravel extending about half way down the 5-km-long Canal as well. *McLean* [1980] and *Martin and Church* [1995] estimated from repeated channel surveys that the average annual deposition in Vedder River is about 50,000 m<sup>3</sup> bulk volume. However, individual major floods are known to be capable of delivering as much as 200,000 m<sup>3</sup> of material.

As the consequence of sediment deposition, Vedder River is a downstream-fining cobble- to pebble-gravel channel flowing on a gradient which declines from  $4.6 \times 10^{-3}$  in the first 3 km to  $1.1 \times 10^{-3}$  at the head of the Canal. Typical grain size declines from about 50 mm immediately below Vedder Crossing to less than 20 mm at the head of the Canal. This appears to be predominantly a sorting phenomenon: Chilliwack River drains a portion of the northern Cascade Mountains which is composed of a wide range of heavily metamorphosed sedimentary and volcanic rocks of Palaeozoic and later age, and some granitic intrusives, so many of the lithologies (e.g., quartzite, diorite, argillite, limestone, and chert) are highly resistant to abrasion.

There are set-back flood dykes over the whole distance, but these do not prevent the channel from adopting a wandering or low-order braided habit, the latter in the less stable reaches near the head of the fan. The mean width is about 100 m in the more stable reaches, and about 250 m in the braided reach. There are no tributaries so, apart from unmeasured seepage, discharge is constant downstream and is derived from the basin of Chilliwack River. The basin experiences infrequent storm-generated high flows in autumn/winter, and more regular snowmelt-generated high flows in spring/summer. In either season the occurrence of rain on snow produces the greatest floods. The highest flows occur in late autumn but are typically of only 1 or 2 days' duration, whereas summer flood stages may persist for many days or even weeks. Between 1977 and 1996, a period of relatively stable hydrological regime on the west coast of North America, the mean winter flood magnitude at Vedder Crossing was 335 m<sup>3</sup> s<sup>-1</sup>, and the mean summer flood magnitude was 220 m<sup>3</sup> s<sup>-1</sup>.

The hydraulic geometry of the channel is known at two sections, Vedder Crossing and Yarrow (sections 1 and 33 in Figure 1). Both sections are relatively narrow and nearly rectangular, unlike most other sections, so width increases relatively little with discharge. Figure 2 shows that flow resistance calculated from these data crosses the trend of a Keulegan-type equation with the SEDROUT default values of  $a = 2.0$  (consistent with a von Karman constant of 0.41) and  $b = 1.1$  (equivalent to a roughness height of  $k_s = 3.11D_{84}$ , as recommended for gravel bed rivers by *Bray and Davar* [1987]). The additional factor indicated by the steeply varying relations at a station is channel form resistance, which is progressively drowned at higher flows. In the present context what matters is the downstream change in resistance at high flow. Figure 2 suggests a high-flow limit of  $b \sim 1.7$  at Yarrow, whereas the equivalent curve for Vedder Crossing suggests  $b \sim 0.5$ . Since 1981, a sequence of 49 monumented cross sections (Figure 1) has been regularly surveyed along Vedder River reach as part of the flood management program of the Water Management Branch, British Columbia Ministry of Environment, Lands and Parks (BCE hereafter). The average distance between survey lines is 170 m, but the actual distance varies along the reach so that a spacing of about 1.5 channel widths is maintained. The 1990 survey provided the cross sections that are used in the simulations and the "current" long profile of the channel bed

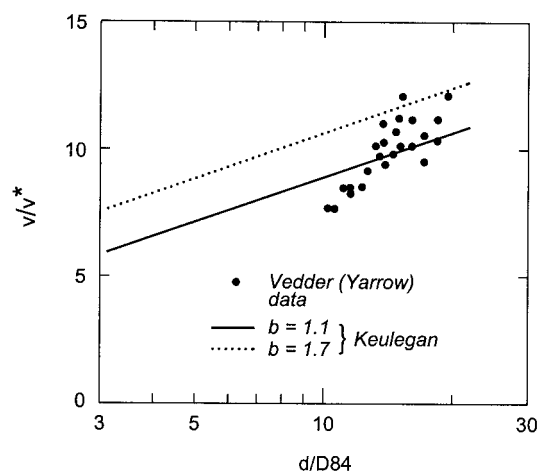


**Figure 2.** Flow resistance at the Yarrow gauge section in Vedder River. For comparison, some Keulegan-type relations are displayed.

(Figure 3), which is based on the mean channel bed elevation at each cross section.

A variety of grain size data is available. The best data for modeling purposes are 19 subsurface bulk samples taken by Y. Martin in 1991 between Vedder Crossing and a point in the Canal 11 km downstream. Most samples were from barhead to midbar locations, but avoiding conspicuously armoured areas. The surface was cleared off before the sample was taken, and sample sizes followed the criteria of *Church et al.* [1987]. The data are displayed by *Martin and Church* [1995, Figure 4]. We supplement these data with samples from the Canal in 1998 [*Bloomer*, 2000] and seven subsurface samples taken by BCE personnel after a major flood in 1989. The BCE samples were truncated at 200 or 250 mm. They should be reliable for estimating  $D_{50}$ , since very little  $>200$  mm material is present in the channel, but only some of them are reliable in the coarse tail. The combined data show general downstream fining beyond about 2 km but no clear trend proximally and substantial scatter throughout (Figure 3). The fitted Sternberg coefficient, i.e., the exponent  $\alpha$  in  $D/D_0 = \exp(-\alpha x)$  where  $D$  is grain diameter and  $x$  is distance downstream, is slightly higher for  $D_{84}$  (0.15) than  $D_{50}$  (0.13).

Annual gravel fluxes in different reaches of Vedder River were estimated by *Martin and Church* [1995] from channel changes between six repeat surveys of the 49 cross sections in the period 1981–1990. Direct measurements of bedload transport were also made at Yarrow between 1971 and 1974. This measurement program was described by *McLean* [1980]. Significant sand transport was found to commence at about 150 m<sup>3</sup> s<sup>-1</sup>, and gravel transport at 225–250 m<sup>3</sup> s<sup>-1</sup>, but substantial quantities of gravel were transported only at flows above 350 m<sup>3</sup> s<sup>-1</sup>. Obtaining a quantitative measure of the transport is difficult because the efficiency of the samplers remains uncertain and the number of samples constituting each measurement was limited. The performance of the same samplers in Fraser River was discussed by *McLean et al.* [1999], and we adopted correction methods similar to the recommendations of those authors except that, for correction of the basket samples, we assumed on the basis of our simulations that 50% of the transported material was finer than the sampler mesh.

*Martin and Church's* [1995] analysis showed that patterns of aggradation and local degradation are spatially variable along

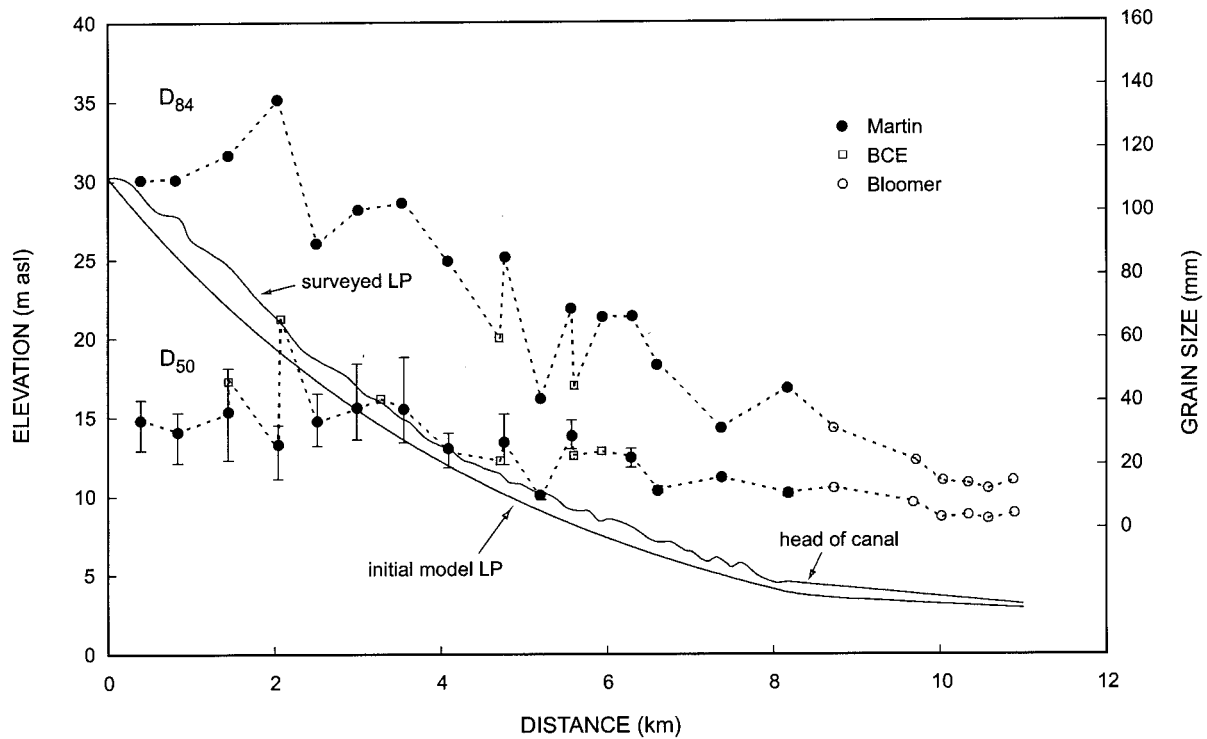


**Figure 3.** Long profile and bed material grain size in Vedder River. Distances are downstream from Vedder Crossing. Smooth profile curve is the initial profile for simulations. See text for sources of grain-size data and calculation of  $\pm 1$  standard deviation error bars.

Vedder River from flood to flood. They are further complicated by periodic removal of gravel to maintain flood capacity. We do not expect to simulate such details because we do not simulate the unsteady flow or sediment delivery to the reach that are associated with such variations, nor the local variability associated with bars, pools, and braiding. Rather, our objective, consistent with the purpose of the model, is to simulate the overall development of the aggrading channel over an extended period of time.

**4. Initial and Boundary Conditions**

In order to run SEDROUT it is necessary to specify channel cross sections, initial long profile and bed GSDs, water discharge, and incoming sediment flux and GSD. These conditions are outlined here. The default choices and alternatives are summarized in Table 1.

**4.1. Initial Conditions**

Modeling was done using approximations of the 49 surveyed cross sections from Vedder Crossing (defined to be at distance 0 m) to the Head of Canal (8175 m). To avoid end effects, the model domain was extended part way down the Canal by adding sections at 200 m intervals to 11,000 m, making a total of 63 sections (Figure 1). For purposes of 1-D modeling, the sections were approximated as rectangular, with banks high enough to prevent overbank flow. This is fairly realistic for the Canal, but surveyed sections upstream of 8175 m are of variable width and often irregular shape. Most simulations were done using the same width at each section, but some used the surveyed widths. In uniform-width runs, width was set at the overall mean of 110 m on the grounds that at wide sections the flow and bedload transport are generally concentrated into a fraction of the total width.

**Table 1.** Default and Alternative Specifications for SEDROUT Simulation Runs in This Paper

Feature	Default Specification	Alternative Specifications Used
Bedload transport	Parker [1990] extended to gravel and sand fractions modified straining function exchange $c = 1$	gravel fractions only using original straining original straining $c = 0$ for sand fractions
Flow resistance	Keulegan with $b = 1.1$	$b = 1.7, b = 0.5, \text{width-dependent } b$
Channel width	uniform	variable
Initial conditions		
Long profile	exponential to 8.2 km, then straight	exponential throughout
Bed GSD	constant to 8.2 km, then fine	stepped fining
Boundary conditions		
Discharge	$350 \text{ m}^3 \text{ s}^{-1}$	250, 300, 400, 450, $500 \text{ m}^3 \text{ s}^{-1}$
Bedload supply	flux and GSD at capacity	flux at capacity but fixed GSD fixed flux and GSD

The initial long profile for most runs is a smooth exponential curve to 8175 m, matched to the modern bed elevation at  $x = 0$  but falling below it thereafter to give up to about 3 m of accommodation space for aggradation. Beyond 8175 m the initial profile straightens to the design slope of  $2.8 \times 10^{-4}$  for Vedder Canal and to a match with our 1998 measurement of bed elevation at 12 km, beyond which aggradation is thought to be negligible. As can be seen in Figure 3, these specifications yield a break of slope at the head of the Canal, and about 1.6 m of accommodation space there. Independence of this assumption was confirmed by doing a run starting from a profile with no break of slope.

Most runs began with a coarse bed GSD everywhere along Vedder River, i.e., no downstream fining. This is unrealistic, but makes it easy to determine when the effect of the initial condition has migrated out of the model domain. The initial GSD was set as the average of the first two measured GSDs below Vedder Crossing truncated at 0.25 mm, below which sand is likely to travel in suspension in high flows. It contains 13% sand, with  $D_{50} = 35$  mm and  $D_{84} = 111$  mm. Two gravel-only runs were done with the GSD truncated at 2 mm, making  $D_{50} = 44$  mm and  $D_{84} = 120$  mm. Preliminary runs used the coarse initial GSD all the way to 11 km, but this was found to inhibit transport in the Canal (which had a fine bed when built in 1928) and cause implausibly high local aggradation at the break of slope. Most runs therefore started with a finer GSD for the Canal, having  $D_{50} = 1$  mm and  $D_{84} = 8$  mm. Independence of initial conditions was confirmed by a run starting from a stepped downstream fining profile.

#### 4.2. Boundary Conditions

The water discharge  $Q$  was assumed steady over time and constant downstream. Adopting a constant discharge for simulations of sediment routing and bed evolution is analogous to the dominant discharge assumption in both empirical and rational approaches to river morphology, and poses the same problem of choosing one point from the magnitude-frequency curve describing the spectrum of flows that shape the river. We mostly used  $Q = 350 \text{ m}^3 \text{ s}^{-1}$ , which is approximately the overall mean annual flood and comfortably above the threshold for gravel movement. This discharge was exceeded for 0.17% of the total time of record after 1976, i.e., 15 hours per year on average. Sensitivity to choice of discharge was assessed by comparative runs with higher and lower values, and the choice is reviewed in our discussion of observed and simulated bedload transport rates.

With constant water discharge the natural upstream boundary condition for sediment flux and GSD is a constant sediment input. However, there are no bedload transport measurements at Vedder Crossing. The stage record of the gauge shows that bed elevation here is fairly stable, reflecting a situation of sediment transmission in the rather narrow channel where the river cuts through the last ridge of the Cascades, with deposition zones upstream and downstream. In general, therefore, we used a fixed-elevation condition for the head of the reach, with the sediment influx and GSD there calculated by the model to match transport capacity. This assumption was also made for Allt Dubhaig by *Hoey and Ferguson* [1994]. It implies that sediment flux decreases, and its GSD becomes somewhat finer, over time as the reach immediately downstream aggrades and the slope and shear stress decline. It can alternatively be argued that the flux and GSD of incoming load at a given flow are constrained by conditions immediately upstream and need

not evolve systematically over time. Some runs were therefore done with a specified GSD, flux, or both for the incoming load. Manipulation of this condition turns out to be critical for obtaining the best downstream-fining fit.

### 5. Basis for Comparison Between Runs and With Field Data

In order to compare one run with another, or with the present-day river, it is necessary to decide what properties to consider and at what time in each simulation. This is difficult because we are attempting to simulate the coevolution of two bed properties (elevation and GSD), starting from an arbitrary initial condition known to be unrealistic and with no equilibrium short of a very long-term end state with no remaining profile concavity or downstream fining. Consequently, we must first run the model to some realistic reference state.

Feeding a capacity or near-capacity sediment load to the head of a concave long profile causes progressive aggradation of the rest of the profile. Whether the simulation starts with no downstream fining or a weakly stepped fining profile, transport over the too-coarse bed is strongly size-selective, so there is a brief period of rapid adjustment during which relatively fine sediment is deposited progressively down the reach, creating a wave-like aggradational front. In uniform-width runs the deposited sediment is finer-grained farther downstream: that is, downstream fining develops. The same general pattern develops in runs with variable width, but the higher shear stress at narrower sections can cause local coarsening and/or degradation. After the fining front has passed through the reach, there is an indefinitely long period of much more gradual evolution during which aggradation is accompanied by slow coarsening of the bed through preferential winnowing of the finer fractions. A typical time sequence is shown in Figure 4. Total volumes of aggradation in each time slice can be computed from the model output and generally decrease through a run.

We chose to continue each run beyond the passage of the fine front until we obtained the best match between the simulated and actual long profiles, then compared the simulated pattern of downstream fining with the observed fining pattern and that in other runs. We selected the long profile as the controlling measure of goodness of fit because we consider it to be the most robustly observed distributed feature of the channel. The comparison with the sediment fining pattern then becomes the test of model performance. Successful simulation of the pattern of downstream fining will establish that the model physics is sufficiently correct and comprehensive and that the model is not specially influenced by the arbitrary initial conditions, so that we are entitled to continue the run from this point with the expectation that the model is performing a realistic simulation. Our procedure is analogous to the standard practice of initializing a model by running it to some equilibrium state except that, in the nature of our problem, there is no equilibrium to be had short of the final end state.

We consider the downstream profiles of both  $D_{50}$  and  $D_{84}$ , using subsurface bulk GSDs rather than pebble-count surface GSDs since the model deals with bulk GSD. It must be recognized that the field data, although based on current best practice [*Church et al.*, 1987], are subject to substantial sampling error. The Monte Carlo results of *Ferguson and Paola* [1997] have been used to assess bias and precision in the field percentiles. The large bulk samples collected by Martin ensure no sampling bias, but precision is low because the bed material is

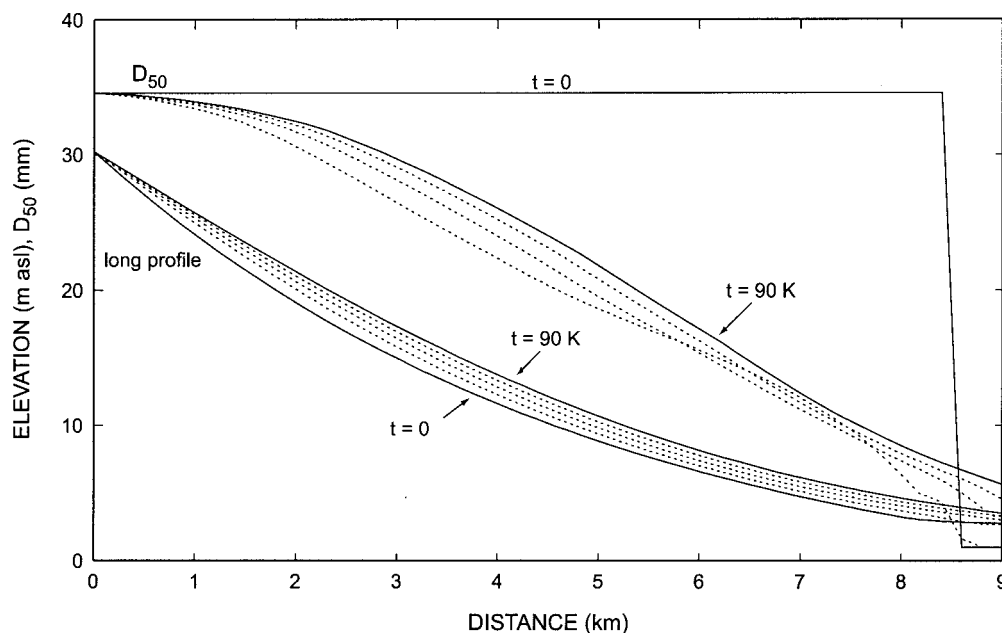


**Figure 4.** Time sequence of long-profile development during a simulation (run 3: see Table 1 for specifications).

poorly sorted (psi standard deviations range from 2.3 to 3.6, apart from one distal site with  $\sigma = 1.3$ ). Standard errors for the median grain size in psi units are about 0.4 in the upper 5 km and 0.2 in the lower 3 km of the river, implying 95% confidence intervals for  $D_{50}$  of about +75%/–40% and +30%/–25% respectively. Standard errors for  $D_{84}$  are much higher, of order 2 at most sites. We therefore trust the medians more for comparison with the model, but use both  $D_{50}$  and  $D_{84}$  and look for the right general pattern of downstream fining rather than a good match with individual fieldsites. The main quantitative criterion used is the root-mean-square difference or error (RMSE) between observed and simulated diameters (expressed in psi units since this equalizes variance along the profile) at 17 of the 18 sites for which GSD data exist close to a model cross section; one bar-tail site noted as anomalous by *Martin and Church* [1995] is excluded. We also consider Sternberg coefficients, but a good match between observed and simulated fining coefficients could occur despite systematic underprediction or overprediction of grain size, so the RMSE is the more robust measure of fit. When interpreting the results it should be noted that the time of best long-profile match was not established accurately because output files were written only at increments of 10% of total run duration; uncertainties of at least 0.01 in RMSE, and at least 5% in aggradation volume, are expected for this reason.

Secondary measures of model performance are then checked by comparing simulated transport rates with indirect estimates of bedload fluxes at intervals along the river [*Martin and Church*, 1995] and bedload measurements at Yarrow [*McLean*, 1980]. There are uncertainties in comparing these with model fluxes, but they provide a direct test of rate of profile development, hence whether the model performs reasonably in time. Only if observed and simulated transport rates are comparable can we assert that the modeled sediment flux is realistic and consider using the model for short-term predictive purposes.

Our sequence of tests was designed first to study aspects of

internal logic in SEDROUT that have not previously been examined; then to examine functional conditions that are selected within the code, particularly flow resistance; and, last, to test sensitivity to the externally specified conditions that are particular to the simulation, including initial long profile, grain size specification, and widths. After arriving at what appears to be the best combination of specifications for running the code, we investigated how the hydrological and sediment-supply forcing affects the ostensible behavior of the river. We repeated most of the runs on two different computer systems. While run times varied according to hardware and compiler, results were identical to within very small computational error margins. The run specifications are given in Tables 1 and 2. The results reported below constitute a sequence of numerical experiments which are described in turn and summarized in Table 2.

## 6. Results

### 6.1. Experiment 1: Specification of Sediment Transport

The first runs (Figure 5) were designed to test the effect of program changes to provide more realistic straining over the various sediment sizes and extend the range of sediment sizes to include sand. The latter is important since it is known that the presence of sand influences gravel mobility [e.g., *Wilcock*, 1998]. Run 1 was a gravel-only simulation employing program options used for modeling Allt Dubhaig. In this simulation there is excessive fining, especially in  $D_{50}$ , so that distal values of  $D_{50}$  are quite severely negatively biased (i.e., simulated diameters are finer than observed).  $D_{84}$  is underestimated to a lesser extent. The exaggerated fining of  $D_{50}$  suggests that transport is selecting too strongly for finer sizes. Adoption in run 2 of the modified straining function discussed in 2.2 reduced the simulated time to match the observed long profile by 50%, indicating a doubling of sediment flux. The fits to the

**Table 2.** Summary Results of SEDROUT Simulation Runs in This Paper

Run	Special Feature of Run	RMSE <sup>a</sup> at Time <i>T</i> of Best Match to Long Profile <sup>b</sup>				Sternberg Coefficient <sup>b</sup>		Aggradation Volume, Mm <sup>3</sup>
		<i>T</i> , kmin	<i>z</i> , m	psi <sub>50</sub>	psi <sub>84</sub>	<i>D</i> <sub>50</sub>	<i>D</i> <sub>84</sub>	
	reference values (exponential fits to data) <sup>b</sup>		0.56	0.33 (*0.31)	0.28 (*0.28)	0.13 (*0.12)	0.15 (*0.15)	
1	gravel only, Parker straining	400	0.55	0.76*	0.40*	0.29*	0.24*	1.61
2	gravel only, Hoey straining	200	0.44	0.57*	0.26*	0.20*	0.22*	1.61
3	default run (as Table 1)	90	0.45	0.38	0.37	0.18	0.10	1.76
4	higher <i>b</i>	120	0.44	0.43	0.34	0.19	0.10	1.73
5	lower <i>b</i>	60	0.47	0.34	0.40	0.18	0.09	1.67
6	smooth initial long profile	100	0.48	0.42	0.35	0.19	0.10	2.04
7	stepped initial fining	90	0.44	0.40	0.36	0.19	0.10	1.82
8	variable width	300	0.72	0.52	0.35	0.19	0.12	2.61
9	variable width and <i>b</i>	180	0.53	0.47	0.34	0.18	0.11	2.78
10	capacity feed, GSD equal to mean bed	(400) <sup>c</sup>	0.47	0.76	0.48	0.19	0.16	1.44
11	capacity feed, GSD finer	120	0.44	0.29	0.41	0.17	0.10	1.78
12	as 11 but fixed flux 0.0015 m <sup>3</sup> m <sup>-1</sup> s <sup>-1</sup>	140	0.47	0.30	0.38	0.18	0.10	1.85
13	as 12 but 0.002 m <sup>3</sup> m <sup>-1</sup> s <sup>-1</sup>	100	0.39	0.37	0.35	0.18	0.10	1.80
14	<i>Q</i> = 250 m <sup>3</sup> s <sup>-1</sup>	160	0.44	0.51	0.30	0.21	0.12	1.71
15	<i>Q</i> = 300	120	0.44	0.43	0.34	0.19	0.10	1.77
16	<i>Q</i> = 400	70	0.46	0.34	0.40	0.17	0.09	1.73
17	<i>Q</i> = 450	60	0.47	0.30	0.43	0.16	0.08	1.78
18	<i>Q</i> = 500	50	0.48	0.28	0.44	0.16	0.08	1.98

<sup>a</sup>RMSE denotes root-mean-square error in elevation *z* or grain size (psi 50 or psi 84).

<sup>b</sup>Starred values are for gravel-only runs, others are for full GSD > 0.25 mm.

<sup>c</sup>Run 10 did not achieve optimum long-profile matching.

long profile, *D*<sub>50</sub> and *D*<sub>84</sub> are all improved compared to run 1, but *D*<sub>50</sub> is still underestimated.

Adoption of a gravel-sand sediment mixture (run 3), simulating the entire bed material distribution in Vedder River, gave as good a long-profile fit but in less than half the time again. The more rapid aggradation is because inclusion of sand in the calculations reduces *D*<sub>50</sub> and thus the reference stress, thereby increasing overall sediment flux and the mobility of coarser fractions in proximal reaches. The simulation of *D*<sub>50</sub> is considerably better in this run, although the Sternberg coefficient still exceeds the observed value by 30%. This is mainly because the field data show no clear fining over the first 3 km. The improved fit to *D*<sub>50</sub> is at the expense of *D*<sub>84</sub> which is now substantially overestimated downstream. We have much more confidence in the precision of observed values of *D*<sub>50</sub> than of *D*<sub>84</sub>, so gravel/sand bed and modified straining were adopted in all subsequent runs.

Runs 1–3 assumed deposition entirely to the surface (*c* = 1 in the fractional continuity equation of Hoey and Ferguson [1994]). A run using *c* = 0 for fractions <2 mm (to mimic sand infiltration into a gravel framework) gave inferior results so *c* was left at 1 and run 3 is used as the reference for goodness of fit.

## 6.2. Experiment 2: Flow Resistance

As noted earlier (Figure 2), the available gauging-station data for Vedder River suggest different high-flow limiting values of *b* in the Keulegan equation than the SEDROUT default value of 1.1. We therefore did runs with the higher value (*b* = 1.7; run 4) indicated by Yarrow measurements and the lower value (*b* = 0.5; run 5) which appears to better fit Vedder Crossing data. The high value corresponds to a halving of *k*<sub>s</sub>/*D*<sub>84</sub> from 3.1 to 1.6 and the low value to a doubling to 6.2. Runs 3–5 collectively show that as *b* increases, the time to match the long profile increases substantially; the long-profile and *D*<sub>84</sub> fits improve slightly; but the *D*<sub>50</sub> fit worsens slightly. Given these trade-offs, and the practical advantage of a stan-

dard flow resistance criterion when the actual relation remains unknown at most places along a river, we did not pursue numerical adjustments of the equation. However, we consider flow resistance again when we take up modified channel width specifications below.

## 6.3. Experiment 3: Effect of Initial Conditions

As outlined above, the initial channel in most runs had breaks of slope and grain size at 8.2 km, and up to 3 m of accommodation space. To check sensitivity to these initial conditions, we did a simulation (run 6) starting from a more concave long profile with no break of slope into the Canal, up to 4 m of accommodation space, and a coarse GSD throughout including the Canal. Another simulation (run 7) started from the default long profile but with a stepped pattern of initial downstream fining. Run 6 took slightly longer to reach the best match to the surveyed long profile, because more aggradation was required, but there was very little difference in goodness of fit at this time: a slight worsening in long-profile RMSE, and slightly higher Sternberg coefficients giving a small deterioration in RMSE for *D*<sub>50</sub> but a small improvement for *D*<sub>84</sub>. The initial fining in run 7 greatly reduced the time required for a smooth downstream fining profile to develop, but the time to best match the surveyed long profile was almost unaffected since it depends mainly on the time to accumulate sufficient sediment. The profile, *D*<sub>50</sub> and *D*<sub>84</sub> fits at that time were close to those in the default run.

These simulations confirm that, so long as the initial profile is more concave than the modern one, sooner or later aggradation will give more or less the same approximation to the modern profile. The existence or not of initial downstream fining is also unimportant; if a fixed-elevation upstream boundary condition is used, all that matters is that initial proximal GSD is realistic. All subsequent results are for the initial profile with break of slope into fine-bed Canal.

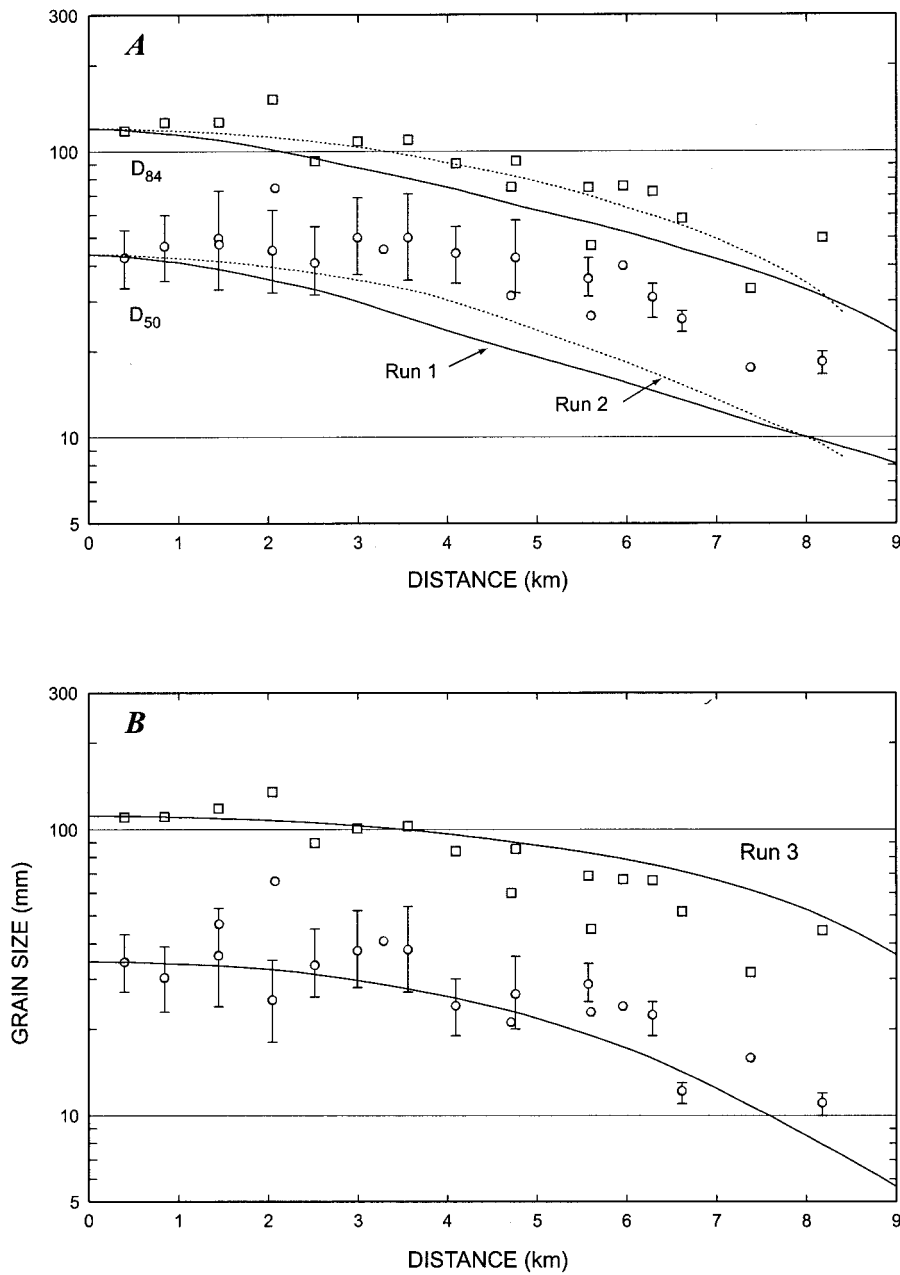


**Figure 5.** Simulated downstream fining profiles for bed material  $D_{84}$  and  $D_{50}$  to test SEDROUT logic. Unconnected symbols represent sediment grain sizes measured in the field, with error bars as in Figure 4. (a) Gravel only runs, compared with observed GSDs, truncated at 2 mm; (b) run for gravel plus sand, compared with observed GSDs truncated at 0.25 mm. Complete specifications of the simulations are given in Tables 1 and 2.

**6.4. Experiment 4: Effect of Width Specification**

SEDROUT is a 1-D model, whereas river channels plainly are 3-D systems. Since flow cross sections must be specified in order to estimate some of the mean hydraulic quantities for 1-D computation, the possibility exists to incorporate some summary effects of the additional system dimensions. This can be done most simply by recognizing the variable width of the channel. Run 8 (Figure 6) studies this. Some approximation of local effects in the pattern of aggradation and downstream fining is induced by the variable width, which feeds back through the hydraulic conditions to affect shear stress locally. There is initial degradation and coarsening in narrower

reaches, and aggradation where the channel widens. Because aggradation is concentrated in the wider sections, the best long-profile fit is not achieved until far more time has elapsed, and more overall aggradation has occurred, than in uniform-width runs. The simulated long profile matches the observed profile extremely well to 2.5 km and from 5 to 8 km, but is below it at 3 to 5 km so that the RMSE is higher than in uniform-width runs despite the visually good fit. The overprediction of downstream fining in  $D_{50}$  also worsens, but the  $D_{84}$  fit is slightly improved; it is visually excellent from 2 to 6 km but there is some overprediction distally and the proximal downstream coarsening is slightly exaggerated.

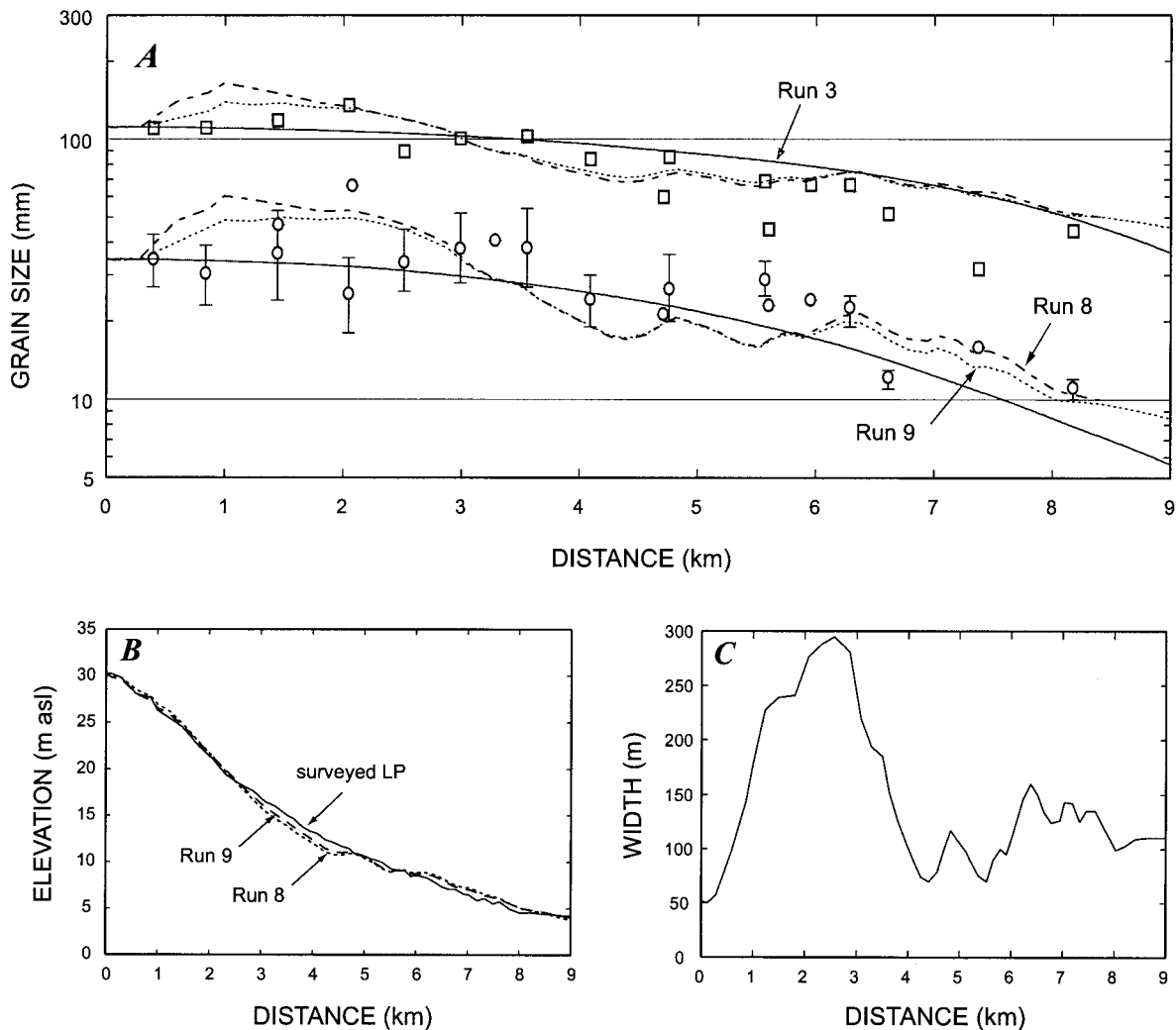


**Figure 6.** Simulated (a) downstream fining and (b) long profiles for runs with variable width (runs 8 and 9) and width-dependent flow resistance (run 9). The reference is run 3. Conventions as in Figure 5b. (c) Widths used are bankfull width at each surveyed section.

It appears then that, while local variations in width may explain some of the observed departures from smooth downstream fining, using the full surveyed width for 1-D calculations does not capture these effects adequately. As noted by Mosley [1983] and Paola [1996], the existence of deep talwegs in braided rivers greatly increases transport capacity over that of the equivalent wide shallow rectangular section. The “hydraulically effective width” concept underlying our uniform-width simulations makes allowance for this phenomenon, though clearly there is scope for further research on ways to allow for lateral variability.

The other aspect of lateral variability in braided reaches is that flow resistance is likely to be higher than in single-thread sections because, even if the effective hydraulic width remains the same, the division of the channel into several functioning sections will preserve a significant measure of form resistance even at high flows. In an attempt to simulate such an effect, run 9 used an inverse linear relation between the  $b$  coefficient in the Keulegan equation and the channel width. The relation was set to give  $b = 1.1$  at  $w = 110$  m, as in uniform-width runs, but decreasing to 0.5 at the widest sections (equivalent to a doubling of  $k_s/D_{84}$ ). This gave an increase to  $b = 1.3$  at the

narrowest sections. In comparison to run 8 there is a considerable improvement in long-profile RMSE, an improvement also in the  $D_{50}$  fit, and almost no change in the  $D_{84}$  fit (Figure 6). The overall performance remains less good than the default run with uniform width, so we did not pursue the variable-width approach further, but the concept of combining it with width-dependent flow resistance shows promise. Further work is needed on how to quantify it.

#### 6.5. Experiment 5: Sensitivity to Bedload Input

The remaining runs considered the effect of forcing conditions, starting with proximal sediment supply. All runs reported so far employed a fixed-elevation upstream boundary condition, so that the flux and GSD of incoming bedload were automatically matched to the transport capacity at the first cross section at each stage in the computation. As discussed above, it can be argued that the input bedload is controlled by upstream conditions and should be treated as fixed for lack of better knowledge. Runs 10–13 explore this type of forcing.

Runs 10 and 11 retained the fixed-elevation condition to the extent that incoming flux is matched to capacity, but with a specified GSD that stays constant over time. In run 10 this

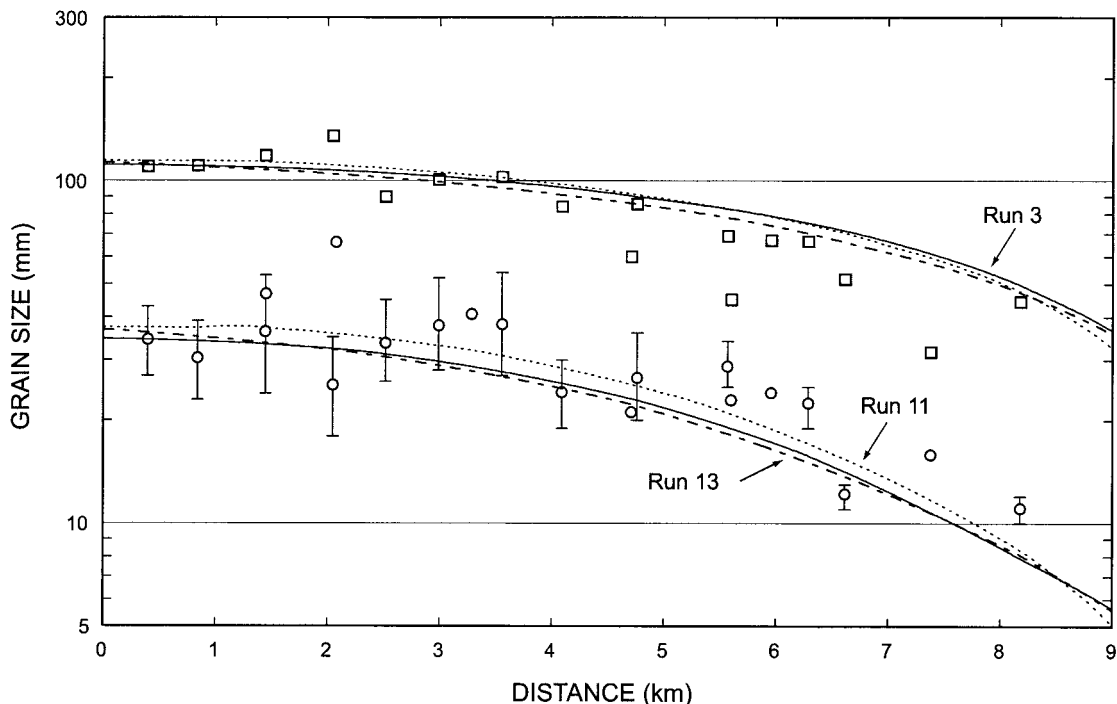


**Figure 7.** Simulated downstream fining profiles with fixed flux (run 13) and GSD (runs 11 and 13) of bedload into the reach. The reference is run 3. Conventions as in Figure 6.

GSD was the average of all the measured subsurface bed GSDs between 0 and 8.2 km, on the assumption that this indicates the long-term supply to the reach. It has  $D_{50} = 25$  mm,  $D_{84} = 91$  mm, and 16% sand. The fixed-elevation constraint forces all this material to be transported into the reach, but the channel immediately downstream is overloaded with coarse fractions and underloaded with fine fractions, leading to downstream coarsening to about 1.5 km. There is a hint in the measured bed GSDs that this effect is real. As a side effect, though, onward transport is greatly reduced so that the midreach aggrades very slowly and there is distal degradation. The long profile never builds up to the observed level, and the overall fits to  $D_{50}$  and  $D_{84}$  are poor, both being overpredicted beyond 2 km.

Run 11 used a somewhat finer feed GSD, based on the average of initial and final feed GSDs in the default run and having  $D_{50} = 18$  mm,  $D_{84} = 83$  mm and 20% sand. With this mix, aggradation was slower overall but by the time of best long-profile match the profile fit was almost identical to that in the default run. The  $D_{50}$  fit was considerably better than the default, the  $D_{84}$  fit slightly worse (Figure 7).

In runs 12 and 13 both flux and GSD of incoming bedload were fixed at constant values. The GSD was as in run 11, and the fluxes were 0.0015 and 0.002  $\text{m}^3 \text{m}^{-1} \text{s}^{-1}$ , respectively. Long-profile matching was naturally achieved sooner at the higher feed rate, but both values gave excellent overall fits. Run 13 in particular had lower RMSE than the default run for all three targets: long profile,  $D_{50}$  and  $D_{84}$  (Figure 7). The improved profile fit is the result of proximal aggradation after brief initial degradation; the slight net aggradation gives a better match to the first 2 km. There is also slight proximal coarsening that assists the fining fits.

These findings led to further sensitivity tests on input GSD and sediment feed rate. In brief, it was found that a shift of

$\pm 10\%$  in the specification of input  $D_{50}$ , without changing the coarse and fine tails, produced variations in the displayed downstream fining that covered the entire range of local variation in the observed values of  $D_{50}$  and  $D_{84}$ , the result varying proportionally downstream with the observed fining (Figure 8a). In comparison, doubling or halving the 0.002  $\text{m}^3 \text{m}^{-1} \text{s}^{-1}$  feed rate produced about  $\pm 4$  mm variation in predicted  $D_{50}$  and about  $\pm 10$  mm in  $D_{84}$ , both results being relatively consistent all the way downstream (Figure 8b). It appears that, with careful tuning of the feed flux and GSD, it would be possible to get an even better overall simulation than run 13.

In sum, this experiment shows that, with low transport rates and variable flows, local bed conditions may not be adjusted to the equilibrium commonly supposed in the sediment transport literature, simply because insufficient time elapses at a fixed flow level for sufficient cumulative transport to effect the adjustment by selective exchange between the load and the bed. This condition identifies, then, a significant forcing that must be tuned for simulations at fixed flow levels beginning from arbitrary bed material specifications.

#### 6.6. Experiment 6: Sensitivity to Discharge Specification

Finally, runs 14–18 assess the effect on profile fit and downstream fining of the choice of steady discharge  $Q$ . Along with the default run they form a sequence from 250 to 500  $\text{m}^3 \text{s}^{-1}$  (Table 2). These flows had return periods from 1.1 to 5.1 years, and durations of 0.70 to 0.05% of the total flow record (61 to 4.4 hours per year), in the 1977–1996 period. Discharge determines the magnitude of sediment transport, hence the time for the long profile to aggrade and downstream fining to develop. The model time to achieve the best match to the observed long profile decreases by 70% as  $Q$  doubles from 250 to 500  $\text{m}^3 \text{s}^{-1}$ . The profile fit at this time worsens slightly as discharge in-

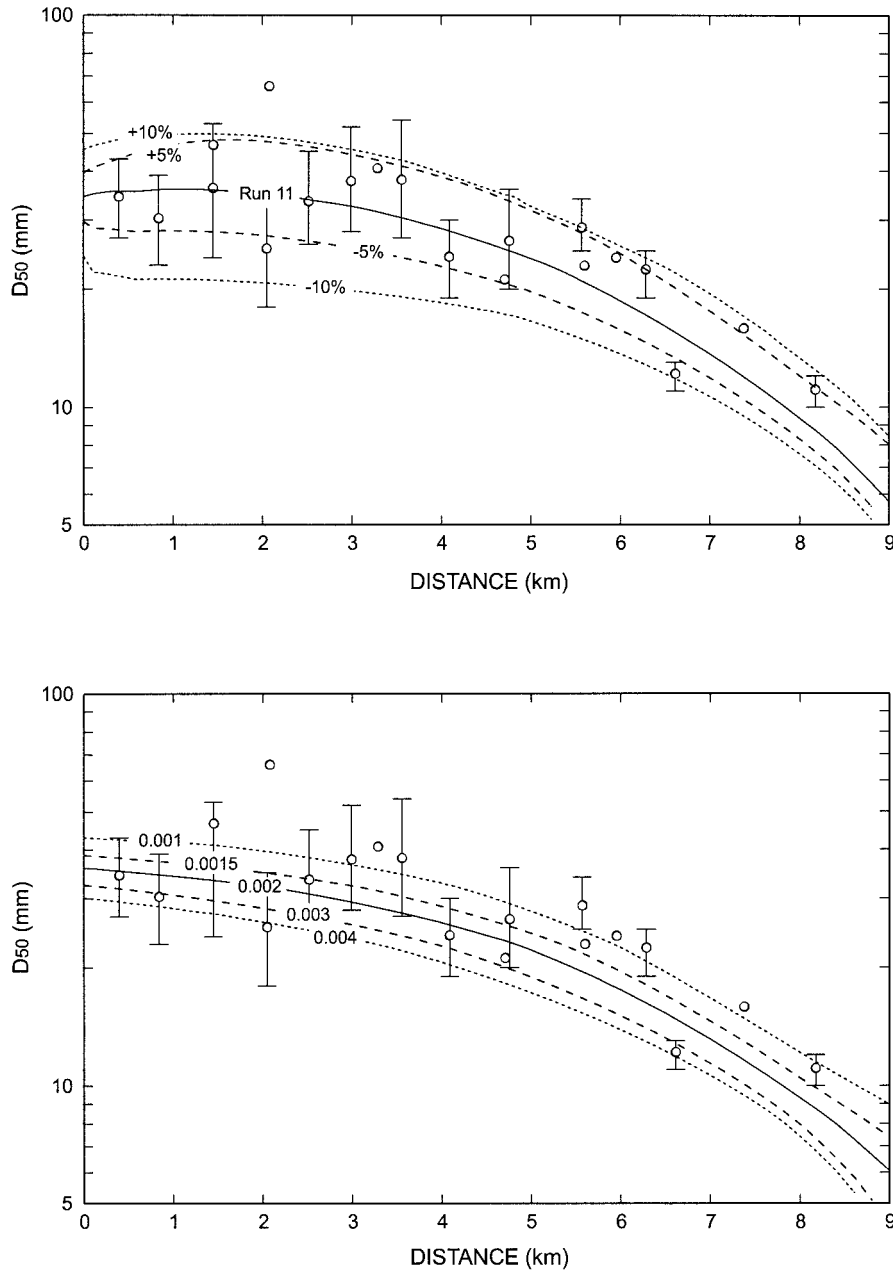


**Figure 8.** Sensitivity tests on the specification of (a) input sediment GSD and (b) sediment feed rate. Conventions as in Figure 6.

creases. The Sternberg fining coefficients for both  $D_{50}$  and  $D_{84}$  decrease progressively with increasing  $Q$  since the distal shear stress becomes higher. This has the effect that higher flows give a better match to  $D_{50}$  but a worse match to  $D_{84}$  (Figure 9). The trends in RMSE cross near the default  $Q$  of  $350 \text{ m}^3 \text{ s}^{-1}$ , but the combined RMSE is almost constant over the full range of flows. The effect of increasing  $Q$  is the same as that of increasing  $\tau_{r50}^*$  or reducing the flow-resistance coefficient  $b$  (i.e., increasing  $k_s/D_{84}$ ) since each causes greater depth and shear stress over a given bed. Thus the results for  $b = 1.7$  and  $b = 0.5$  at  $Q = 350 \text{ m}^3 \text{ s}^{-1}$  are very similar to those for  $Q = 300$  and  $400 \text{ m}^3 \text{ s}^{-1}$ , respectively, at  $b = 1.1$ .

The test shows definitively that no flow specification recreates both the median and the coarse tail of the observed bed material GSD under equilibrium assumptions and when using

uniform active width. The downstream GSD is distorted by the choice of flow level, unless presumably there is a compensating adjustment of input sediment grain size. The inability to match both  $D_{50}$  and  $D_{84}$  well at a single discharge possibly casts doubt on the reliability of the bedload transport equations used, but may simply be because  $D_{84}$  is determined by higher flows than  $D_{50}$ . For practical purposes, it is reassuring that the choice of discharge is not critical.

## 7. Confirmation of the Model

We argued above that the realism of simulations of downstream fining in an aggrading river can be assessed by asking how closely the long profile can be matched at some time in a simulation, and how well the observed pattern of downstream

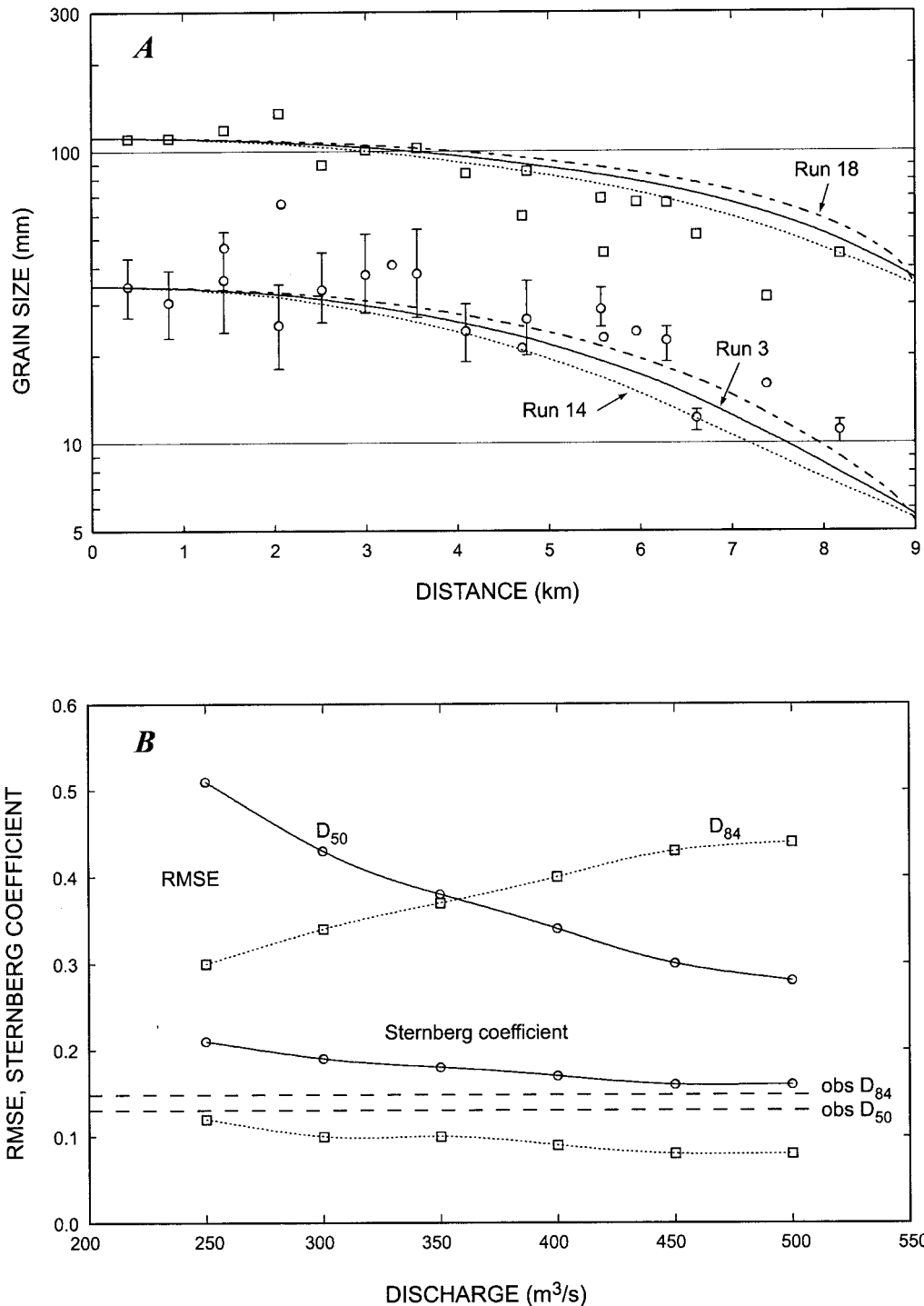


**Figure 9.** Effect of discharge specification on simulated downstream fining: (a) fining profiles, with conventions as in Figure 6. Runs 14 ( $250 \text{ m}^3 \text{ s}^{-1}$ ) and 18 ( $500 \text{ m}^3 \text{ s}^{-1}$ ) are shown, together with the reference run 3 ( $350 \text{ m}^3 \text{ s}^{-1}$ ). Runs 15–17 plot between those shown. (b) Sternberg coefficients and RMS error in prediction of  $D_{50}$  and  $D_{84}$ .

fining (exemplified in this paper by comparisons with field  $D_{50}$  and  $D_{84}$ ) is reproduced at that time. When this general approach is applied to our SEDROUT simulations of Vedder River, the Sternberg coefficients reveal a tendency for the model to overestimate the strength of fining in subsurface  $D_{50}$  but underestimate that in  $D_{84}$ . However, as previously noted, the observed fining profile does not follow Sternberg's law in

the first few kilometers, and the RMSE is a more robust measure of fit. The best simulations fit the observed long profile better than a smooth curve does, and give low RMSE for both  $D_{50}$  and  $D_{84}$ . However, while tests like this indicate the ability of a model to predict features of interest, they do not validate it as physically realistic; good profile and fining fits might be obtained for the wrong reasons [Oreskes *et al.*, 1994]. Stronger

confirmation of the internal workings of a sediment routing model can be obtained only by comparing simulated process rates with those measured in the field.

The best available spatially distributed test is provided by the 1981–1990 gravel budget of *Martin and Church* [1995] and the estimates they derived from it of gravel fluxes at 11 points along the river. This 9-year period included 17 competent floods with a mean annual maximum of  $373 \text{ m}^3 \text{ s}^{-1}$  and an overall peak of  $647 \text{ m}^3 \text{ s}^{-1}$ , so it was hydrologically representative. The gravel budget was based on bulk volumes of channel change, corrected for borrowing and converted to fluxes assuming a porosity of 0.25 and no more gravel flux into Vedder Canal than necessary to avoid negative estimated fluxes upstream. After adjusting the figures to the porosity of 0.3 used in our modeling, the 9-year mean gravel input to Vedder River is  $34,000 \text{ m}^3 \text{ yr}^{-1}$ , nearly all of which is deposited before the Head of Canal. This estimate is supported by a very similar value for the bedload output from the Chilliwack basin upstream of Vedder Crossing [*Ham and Church*, 2000].

In order to compare the field results with fluxes simulated by the model we have to convert one to the same basis as the other. The model assumes continuous high flow, whereas in the real world gravel moves for only a few hours or days per year. We have accordingly adjusted the field results using the long-term duration of all competent flows (taken as  $Q \geq 250 \text{ m}^3 \text{ s}^{-1}$ , with duration 0.7%). Our reasoning is that the steady flow in the model represents the integrated effect of a spectrum of actual flows above this threshold. To confirm this, we calculated the integrated effect of different discharges by weighting the sediment fluxes in model runs at different discharges according to flow duration. The weighted-average flux is very close to the flux for  $Q = 350 \text{ m}^3 \text{ s}^{-1}$ , as used in most of our simulations, and shows that this was an appropriate choice of discharge.

The field estimates of gravel flux, converted in this manner to mean rates during competent flow, are compared in Figure 10 with rates in two simulations: one (run 3) using uniform width, the other (run 9) using variable width. When width-integrated rates are considered, run 3 results plot close to the field data almost to the end of the reach, whereas run 9 underestimates the field data by about 50%. However, when transport per unit width is considered, field data show a systematic downstream pattern of strong decrease, partial recovery, then progressive decline which is not reproduced at all by the uniform-width run 3 but is matched quite well by run 9. Evidently, the two types of simulation each capture some aspects of the observed behavior, but neither captures all aspects. Both simulations pass more bedload to the Canal than *Martin and Church* [1995] assumed. In this respect, the model may be more accurate than the sediment budget result: our survey of the Canal in 1998 showed considerable aggradation, with doubling of the gradient and a gravel front extending almost to 11 km [*Bloomer*, 2000].

The other available comparison is with the bedload transport measurements from the railway bridge at Yarrow (section 33 in Figure 1) reported by *McLean* [1980]. The estimated total ( $>0.25 \text{ mm}$ ) transport rate is plotted against discharge in Figure 11, together with simulated rates at the time of best long-profile match in several model runs. The field values are seen to be almost an order of magnitude lower than the simulated rates, even though the model underpredicts the gravel budget at this point. The discrepancy is somewhat smaller for variable-width runs (8 and 9), but remains large in simulations with

lower discharges, partly because the simulated bed is finer which tends to increase the flux.

Collectively, there is only partial agreement between model simulations and field-derived gravel-budget fluxes and sampler measurements of bedload. It appears that there are problems with one or more (perhaps all) of the sampler measurements, the choice of active width for modeling in the absence of means of allowing for lateral variation, and the representation of gravel/sand transport rates and sorting processes in our modification of the ACRONYM equations.

## 8. Summary and Conclusions

1. In this paper we have applied an enhanced version of *Hoey and Ferguson's* [1994] 1-D fluvial sedimentation model (SEDROUT) to a Canadian gravel bed river of intermediate size. Our initialization and test procedures are considerably more rigorous than any, to our knowledge, previously applied to such a model. In particular, we introduce quantitative criteria for goodness of fit and propose a procedure for model testing when there is no obvious equilibrium endpoint of the simulation. The main findings are as follows. Some of them are explicitly generic suggestions about sediment routing models as a class, and those which apply in the first place to SEDROUT and Vedder River may well be transferable to other models and other rivers.

2. Comparing observed and simulated downstream fining profiles is potentially arbitrary because the simulated profile alters progressively over time. When simulations are started from a profile that allows accommodation space for aggradation, results are essentially independent of initial conditions so long as comparison with GSD data is made at the time when the best long-profile fit is attained. This is proposed as a reasonable solution to the problem of how and when to test a time-dependent model that has no equilibrium except in the very long term. For application of the model to study actual historical sequences of channel development, it would be highly desirable to know the initial as well as final long profile and fining profile, otherwise there is no guarantee that the combination of initial conditions will produce simultaneous convergence of all test conditions to the final observed state of the system. However, some indication of how model time from an arbitrary initial condition converts to real time can be obtained by considering the cumulative aggradation rate and the duration of competent flow.

3. Using this approach, SEDROUT gives good visual and quantitative agreement with the mean trend of gravel/sand accumulation along a river aggrading toward a local base level. This supports and strengthens the encouraging results from the original application to a much smaller stream, and from *Talbot and Lapointe's* [2001] application to a degrading reach.

4. The extension of the model to gravel/sand mixtures suggests that *Parker's* [1990] bedload transport algorithm, developed for gravel only, works satisfactorily for gravel bed channels with some sand so long as a modification is made to the part of the algorithm that allows for differences in bed sorting. Without this, transport predictions can behave counterintuitively. With the modification, downstream fining develops more quickly and remains weaker than when only gravel is considered. The acceleration is partly because the newly included sand is the most mobile part of the bed, but there is also a relative-size effect whereby adding sand makes the gravel more mobile by reducing the bed  $D_{50}$  and threshold shear

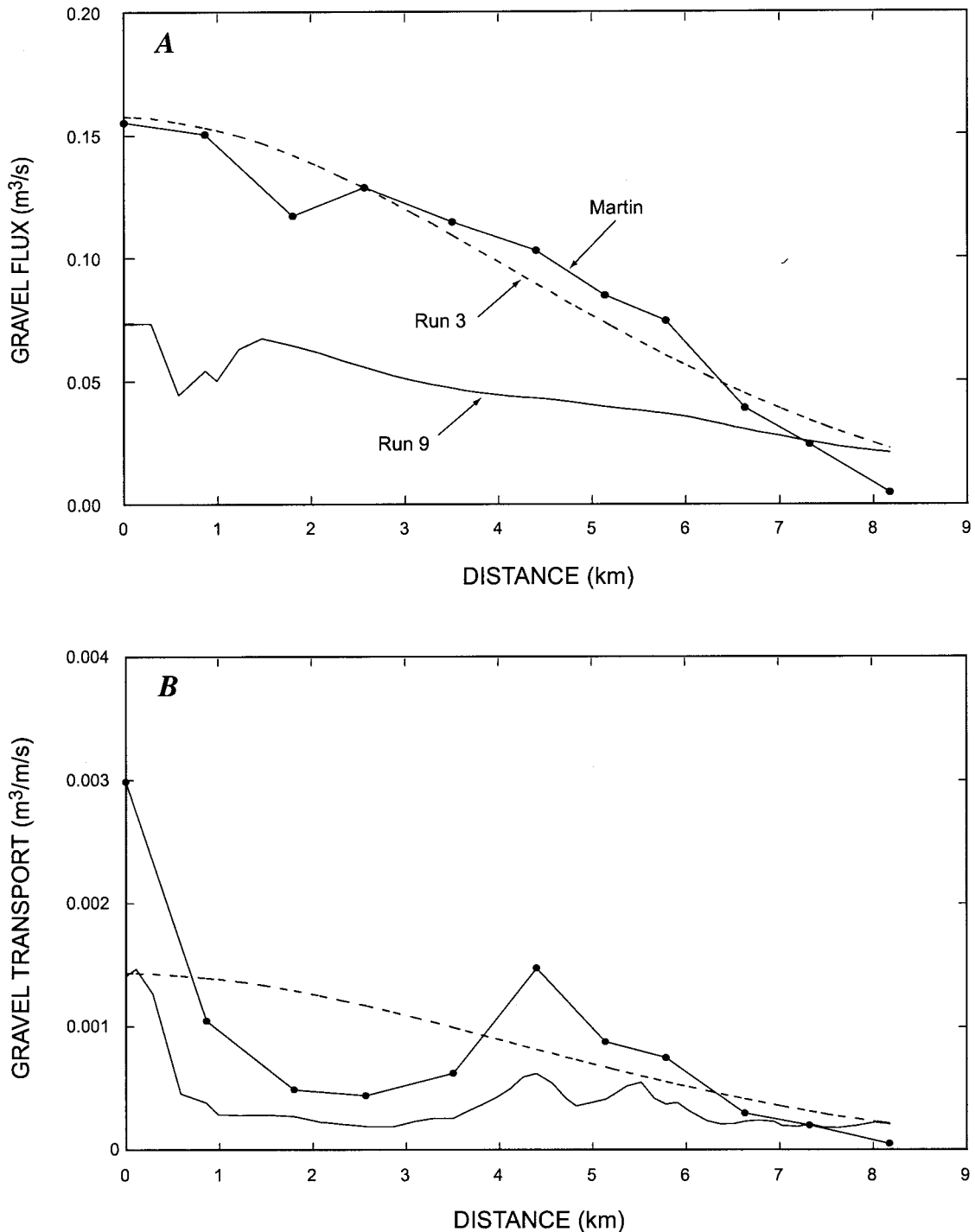


**Figure 10.** Observed and simulated bedload transport rates, integrated across the channel (upper plot) and per unit width (lower). Observed rates based on *Martin and Church* [1995] as discussed in text; simulated rates shown for runs with uniform (run 3) and variable (run 9) width.

stress. Gravel-only simulations substantially overestimate the strength of downstream fining, leading to excessively fine GSDs in the downstream part of the profile, whereas inclusion of sand increases the mobility of coarser gravel (Figure 5). This leads in fact to overestimates of  $D_{84}$  in the distal part of the reach, but the main part of the simulated bed GSD is more realistic.

5. Adjustment of flow resistance coefficients made surpris-

ingly little difference in the strictly 1-D experiments, and the effect is indistinguishable from adjustments of discharge. Inasmuch as we do not know the most effective equivalent discharge in Vedder River (or almost any other river), but generally know a good deal more about the range of discharge than about downstream variations in flow resistance, manipulation of discharge appears to be the most reasonable approach to simulation. On our experience, then, adoption of a general

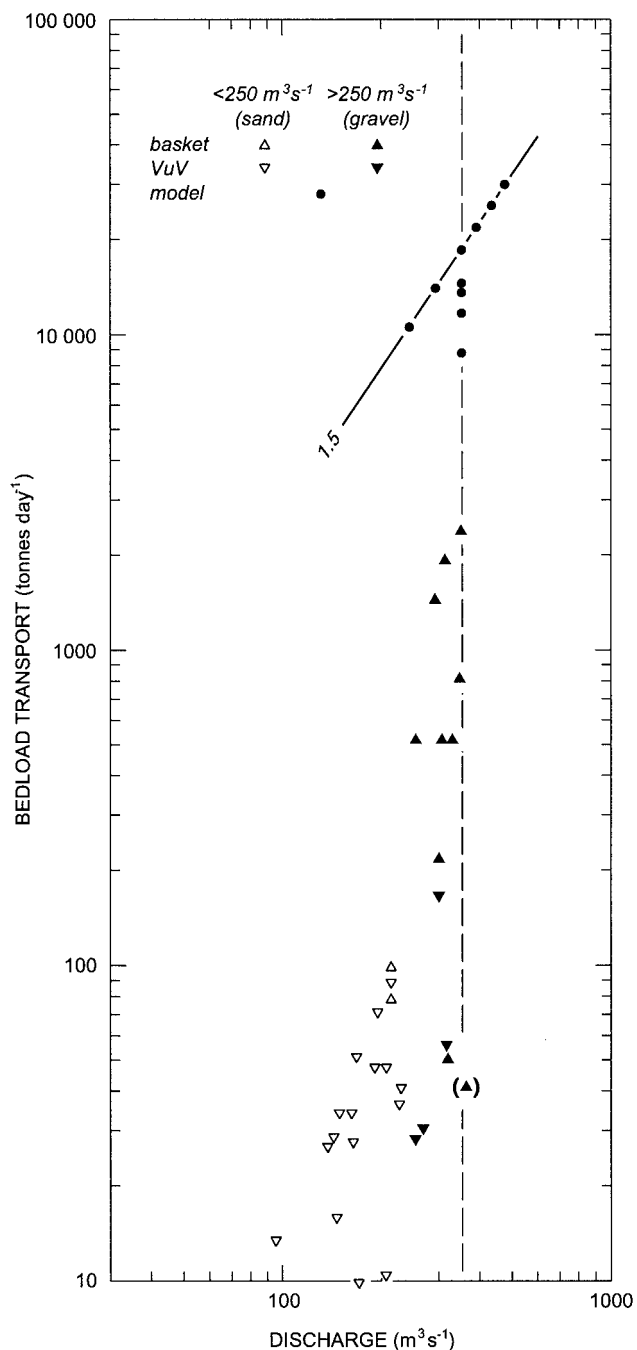


**Figure 11.** Observed and simulated bedload transport rates ( $>0.25$  mm, per unit width) at Yarrow (section 33 in see Figure 1). Data from McLean [1980, Table 22], corrected for sampler efficiency as discussed in text. Simulated results from selected runs as specified in Table 2.

Keulegan-type equation is both expedient and appropriate in this type of modeling.

6. Appropriate specification of the initial bed GSD is important if a fixed-elevation upstream boundary condition is adopted in a sediment routing model, and is difficult because of the well-known local variability of fluvial sediment deposits. In the present application an averaged representation of the two samples from within the proximal 5% of the study reach yielded reasonable results. This is perhaps not surprising since

these samples must represent material that has been transported into the reach. More generally, both the local variability and the sampling error in field estimates of GSD percentiles constrains the testability and predictive accuracy of sediment routing models.

7. Vedder River is typical of many gravel bed rivers in having highly variable width. The choice of a uniform effective width, or variable width, for a 1-D simulation makes a definitive difference to the results since it determines whether or not local variability of bed GSD can be simulated. We found that the direct effect of width variations on depth and therefore shear stress is important (Figure 6). The expected effect of width variation on resistance to flow is more subtle, but a preliminary simulation with width-dependent resistance gave results that suggest this approach should be explored further.

8. It is not self-evident that, for some specified flow, the input sediment transport is necessarily in equilibrium with the hydraulic conditions. For realistic simulations it may be necessary to specify independently the input bedload GSD and perhaps also the flux (or alternatively to consider complete simulation of historical flow sequences with time-varying flow, an exercise that lies beyond the scope of our present investigation). A fixed-feed simulation gave the best overall results of any reported here (Figure 7), even without much attempt at tuning the fit, but we did learn that this is a sensitive adjustment (Figure 8). This too constrains the testability and predictive accuracy of sediment routing models, since sediment feed is seldom known at all reliably.

9. The effect of altering discharge in any sediment routing model is to change the progress of downstream sediment transport and fining. In this study, flows below the reference simulation ( $350 \text{ m}^3 \text{ s}^{-1}$ ) are nearer the threshold for significant gravel transport, so produce slower aggradation but stronger downstream fining (Figure 9). Higher discharge speeds the development of the sediment pile as the consequence of increased transport, but beyond  $400 \text{ m}^3 \text{ s}^{-1}$  it has little effect on the fining trend, presumably because transport is only weakly size-selective at such high flows. The fit to  $D_{50}$  improves, but that to  $D_{84}$  worsens, as discharge increases. The best compromise in our study was a discharge close to the mean annual flood. This has been regarded as a good choice of channel-forming discharge by many previous workers, and turns out to be close to the duration-weighted effective flow for bedload transport at the head of the study reach according to model simulations. However, the simulation results for a given discharge depend on the choice of threshold stress ( $\tau_{r50}^*$ ) and flow resistance ( $b$ ), which were left here at default values for lack of clear evidence to the contrary. Changes in these parameters would confound the effects of changes in discharges; for example, a higher threshold stress, to allow for bed structuring, would imply a higher dominant discharge.

10. Finally, it must be recognized that a good match between observed and simulated channel properties does not constitute strong validation of the physics assumed in a model of this class. If possible, observed and predicted transport rates should be compared for a stronger test. In the present case the simulated aggradation rate is in broad agreement with available field data. Nevertheless, there remains room for further development of 1-D representations of sediment transport physics in order to better accommodate varying combinations of flow, mobilized GSD, and transport in channels with non-rectangular sections. Given the lack of consideration to the effects of local spatial variability in shear stress or grain size, or

temporal variability in discharge, we find the results of the 1-D simulations encouraging and think they offer a good basis for applied work. However, our modification of Parker's [1990] straining function is ad hoc, and independent testing of it would be useful. Furthermore, the inability of the model to estimate realistic flux rates along the whole length of the river or to simultaneously match the fining trends in  $D_{50}$  and  $D_{84}$  suggests the transport submodel is imperfect, probably through some combination of inadequate consideration of surface structuring and coarsening (i.e., hiding) effects and insufficient allowance for lateral variability.

**Acknowledgments.** This project was initiated under a NATO Scientific Exchange Agreement between Ferguson and Church (award CRG961171 to Ferguson). Continuing work was facilitated by a research grant from the Natural Sciences and Engineering Research Council of Canada to Church and by a contract to Church from the British Columbia Ministry of Environment, Lands and Parks for development of a long-range management plan for the gravel-bed reach of Fraser River. We wish to thank Gary Parker for confirming our understanding of his "straining function"; Trevor Hoey for his modification to this function, other coding improvements in 1997/1998, and comments on a draft version of this paper; Dan Bloomer for sharing some of his unpublished Vedder Canal data; Christopher Ayles and Brett Eaton for results on the sensitivity of the simulations to GSD specifications; Paul Jance for some of the figures; and the journal reviewers and editors for suggesting improvements to the wording and raising important issues about what constitutes novelty in a modeling paper.

## References

- Ashworth, P. J., and R. I. Ferguson, Size-selective entrainment of bedload in gravel bed streams, *Water Resour. Res.*, 25, 627–634, 1989.
- Bloomer, D. J., Sediment sorting in the gravel-sand transition along rivers: A field and modelling investigation, Ph.D. thesis, Sheffield Univ., Sheffield, England, 2000.
- Bray, D. I., and K. S. Davar, Resistance to flow in gravel-bed rivers, *Can. J. Civ. Eng.*, 14, 77–86, 1987.
- Church, M. A., D. G. McLean, and J. F. Wolcott, River bed gravels: Sampling and analysis, in *Sediment Transport in Gravel-Bed Rivers*, edited by C. R. Thorne, J. C. Bathurst, and R. D. Hey, pp. 43–88, John Wiley, New York, 1987.
- Cui, Y., G. Parker, and C. Paola, Numerical simulation of aggradation and downstream fining, *J. Hydraul. Res.*, 34, 185–204, 1996.
- Ferguson, R. I., and C. Paola, Bias and precision of percentiles of bulk grain size distributions, *Earth Surf. Processes Landforms*, 22, 1061–1077, 1997.
- Ham, D., and M. Church, Bed material transport estimated from channel morphodynamics: Chilliwack River, British Columbia, *Earth Surf. Processes Landforms*, 25, 1123–1142, 2000.
- Hoey, T. B., and R. Ferguson, Numerical simulation of downstream fining by selective transport in gravel bed rivers: Model development and illustration, *Water Resour. Res.*, 30, 2251–2260, 1994.
- Hoey, T. B., and R. I. Ferguson, Controls of strength and rate of downstream fining above a river base level, *Water Resour. Res.*, 33, 2601–2608, 1997.
- Kuhnle, R. A., Incipient motion of sand-gravel mixtures, *J. Hydraul. Eng.*, 119, 1400–1415, 1993.
- Martin, Y., and M. Church, Bed-material transport estimated from channel surveys: Vedder River, British Columbia, *Earth Surf. Processes Landforms*, 20, 347–361, 1995.
- McLean, D. G., Flood control and sediment transport study of the Vedder River, M.A.Sc. thesis, 282 pp., Univ. of B. C., Vancouver, B. C., Canada, 1980.
- McLean, D. G., M. Church, and B. Tassone, Sediment transport along lower Fraser River, 1, Measurements and hydraulic computations, *Water Resour. Res.*, 35, 2533–2548, 1999.
- Mosley, M. P., Response of braided rivers to changing discharge, *J. Hydraul. N. Z.*, 22, 18–67, 1983.
- Oreskes, N., K. Shrader-Frechette, and K. Belitz, Verification, validation and confirmation of numerical models in the earth sciences, *Science*, 263, 641–646, 1994.
- Paola, C., Incoherent structure: Turbulence as a metaphor for stream braiding, in *Coherent Flow Structures in Open Channels*, edited by P. J. Ashworth, J. L. Best, and C. Bristow, pp. 705–723, John Wiley, New York, 1996.
- Parker, G., Surface-based bedload transport relation for gravel rivers, *J. Hydraul. Res.*, 28, 417–436, 1990.
- Parker, G., and A. J. Sutherland, Fluvial armor, *J. Hydraul. Res.*, 28, 529–544, 1991.
- Parker, G., P. C. Klingeman, and D. G. McLean, Bedload and size distribution in paved gravel-bed streams, *J. Hydraul. Div. Am. Soc. Civ. Eng.*, 108, 544–571, 1982.
- Talbot, T., and M. Lapointe, Numerical modeling of gravel bed river response to large-scale meander rectification: The coupling between the evolution of bed pavement and long profile, *Water Resour. Res.*, in press, 2001.
- van Niekerk, A., K. R. Vogel, R. L. Slingerland, and J. S. Bridge, Routing of heterogeneous sediments over movable bed: Model development, *J. Hydraul. Eng.*, 118, 246–261, 1992.
- Wathen, S. J., R. I. Ferguson, T. B. Hoey, and A. Werritty, Unequal mobility of gravel and sand in weakly bimodal river sediments, *Water Resour. Res.*, 31, 2087–2096, 1995.
- Wilcock, P. R., Experimental investigation of the effect of mixture properties on transport dynamics, in *Dynamics of Gravel-Bed Rivers*, edited by P. Billi et al., pp. 109–139, John Wiley, New York, 1992.
- Wilcock, P. R., Critical shear stress of natural sediments, *J. Hydraul. Eng.*, 119, 491–505, 1993.
- Wilcock, P. R., Two-fraction model of initial sediment motion in gravel-bed rivers, *Science*, 280, 410–412, 1998.
- M. Church, Department of Geography, University of British Columbia, Vancouver, British Columbia, Canada V6T 1Z2. (mchurch@geog.ubc.ca)
- R. I. Ferguson, Department of Geography, Sheffield University, Sheffield S10 2TN, England, UK. (r.ferguson@sheffield.ac.uk)
- H. Weatherly, Kerr Wood Leidal Associates, North Vancouver, British Columbia, Canada V7M 1T3.

(Received August 4, 2000; revised July 25, 2001; accepted August 16, 2001.)

